Green Chemistry

PAPER

View Article Online
View Journal

Cite this: DOI: 10.1039/c4gc01411a

Olefin epoxidation with hydrogen peroxide using octamolybdate-based self-separating catalysts†

Ming-Dong Zhou,*[a,b] Mei-Ju Liu,[a] Liang-Liang Huang,[a] Jian Zhang,[a] Jing-Yun Wang,[b] Xue-Bing Li,[c] Fritz E. Kühn*[b] and Shu-Liang Zang[a]

Received 24th July 2014,
Accepted 18th October 2014

DOI: 10.1039/c4gc01411a

www.rsc.org/greenchem

$Mo_8O_{26}^{4-}$ based organic polyoxomolybdate salts of general formula $[Hmim]_4Mo_8O_{26}$ (Hmim = 1-hexyl-3-methylimidazolium), $[Dhmim]_4Mo_8O_{26}$ (Dhmim = 1,2-dimethyl-3-hexylimidazolium) and $[Hpy]_4Mo_8O_{26}{\cdot}H_2O$ (Hpy = 1-hexylpyridinium) have been prepared and characterized. These compounds were applied as catalysts for olefin epoxidation using hydrogen peroxide (H_2O_2) as oxidant in CH_3CN. The polyoxomolybdate salts exhibit excellent catalytic performance and are also self-separating, a great advantage for catalyst recycling. The catalysts can be reused for at least 10 runs without significant loss of activity.

Introduction

Epoxides are very important key raw materials for a wide variety of chemicals such as glycols, glycol ethers, alkanolamines, and polymers.[1] So far, various compounds including inorganic metal oxides and organometallic compounds have been applied as catalysts for olefin epoxidations using oxygen, ozone, hydrogen peroxide or organic peroxides as oxidants.[2] In particular, hydrogen peroxide-based catalytic epoxidation has received much attention since hydrogen peroxide is a cheap, mild and environmentally benign reagent that produces only water as by-product.[3] Today, H_2O_2 has already been successfully used in industry for propylene epoxidation using TS-1 zeolite as heterogeneous catalyst.[4] However, in the case of homogeneous catalysis, although some molecular organometallic compounds such as CH_3ReO_3 (MTO),[5] $MoO_2X_2L_2$,[6] Cp^*MoO_2Cl[7] *etc.* have proven to be excellent catalysts for epoxidations on a laboratory scale, they are not applied in larger scale industrial processes since these types of organometallic catalysts are rather expensive to produce and their reusability in an industrial-scale process is so far not convincingly established.[8]

Polyoxometalates (POMs), owing to their good catalytic features such as high activity and selectivity, controllable redox and acidic properties at atomic or molecular levels, have also been studied as oxidation catalysts in the past few decades.[9] Among various POMs, the classic Ishii-Venturello system has attracted much interest in oxidation reactions and has been extensively investigated.[10] In the Ishii-Venturello system, the Venturello anion ($\{PO_4[WO(O_2)_2]_4\}^{3-}$) is combined with a quaternary ammonium cation in the formation of an inorganic–organic hybrid salt, which can be used as a phase transfer catalyst using H_2O_2 as primary oxidant for epoxidation of various olefins under rather mild conditions.[11] It has additionally been found that some Keggin- or Lindqvist-type hybrid POMs such as $[C_n mim]PW_{12}O_{40}$ and $[C_n mim]W_6O_{19}$ can also be used as catalysts for oxidations and esterifications.[12]

Despite these catalysts showing high activity towards epoxidations, it is not convenient to separate such catalysts in a homogeneous system. Xi *et al.* have developed an interesting "reaction-controlled phase-transfer catalysis" system using $[\pi\text{-}C_5H_5NC_{16}H_{33}]_3[PO_4(WO_3)_4]$ as a phase transfer catalyst for propylene epoxidation, and the system was also proven to be active for other olefins.[13] In Xi's system, the catalyst precursor is insoluble, but the active species formed is soluble in the reaction medium, and therefore the system manifests a solid–liquid–solid phase transfer of the catalyst during the reaction. Thus the catalyst is "self-separating" after the completion of the reaction and can be recycled simply by filtration.[13] Subsequently, it was found that $PW_{12}O_{40}^{3-}$ or $PO_4[(WO(O_2)_2]_4^{3-}$ anion-based compounds also show self-separation phenomena in catalysis.[14] These kinds of catalysts combine the advantages

[a]School of Chemistry and Material Science, Liaoning Shihua University, Dandong Road, No. 1, Fushun 113001, China. E-mail: mingdong.zhou@lnpu.edu.cn; Fax: +86 24 56863837; Tel: +86 24 56860770
[b]Molecular Catalysis/Chair of Inorganic Chemistry, Catalysis Research Center, Technische Universität München, Ernst-Otto-Fischer-Strasse 1, D-85747 Garching bei München, Germany. E-mail: fritz.kuehn@ch.tum.de; Fax: +49 89 289 13473; Tel: +49 89 289 13096
[c]Key Laboratory of Biofuels, Qingdao Institute of Bioenergy and Bioprocess Technology, Chinese Academy of Sciences, Qingdao 266101, China. E-mail: lixb@qibebt.ac.cn; Fax: +86 532 80662778; Tel: +86 532 80662757

† CCDC 997672 and 997673. For crystallographic data in CIF or other electronic format see DOI: 10.1039/c4gc01411a

of both homogeneous and heterogeneous catalysts; thus they are very promising catalysts for industrial applications.[15]

Recently, we have found that alkylimidazolium/alkylpyridinium octamolybdates exhibit high activity towards olefin epoxidations when using 30% H_2O_2 as oxidant. Moreover, these compounds display self-separation properties in catalysis, and the catalysts can be used at least 10 times without significant loss of activity, indicating good catalyst stability. $Mo_8O_{26}^{4-}$ based salts are types of cheap and easily prepared POM materials.[16] However, not much work has been done with respect to their catalytic performance so far,[17] and almost no studies have targeted their self-separating property. Although Deng *et al.*[17a] have mentioned that $[(n\text{-}C_4H_9)_4N]_4[\alpha\text{-}Mo_8O_{26}]$ could be self-precipitating in a sulfide oxidation catalytic system, ethyl acetate had to be added to precipitate the catalyst. In this work, a highly efficient, "green" method, allowing for good catalyst recycling for olefin epoxidations using 30% aqueous hydrogen peroxide as oxidant and alkylimidazolium or alkylpyridinium octamolybdates as catalysts, is presented.

Results and discussion

Synthesis and characterization

Three $Mo_8O_{26}^{4-}$ based organic polyoxomolybdate salts of formula $[Hmim]_4Mo_8O_{26}$ (Hmim = 1-hexyl-3-methylimidazolium), $[Dhmim]_4Mo_8O_{26}$ (Dhmim = 1,2-dimethyl-3-hexylimidazolium) and $[Hpy]_4Mo_8O_{26}\cdot H_2O$ (Hpy = 1-hexylpyridinium) have been synthesized. The structures are shown in Scheme 1.

All three compounds were characterized by FT-IR, ^1H NMR, ESI MS (positive mode) and elemental analysis (see Experimental section). The melting point and decomposition temperature were determined with a micro-melting point apparatus and by thermogravimetric analysis (TGA). All three compounds are not conventional ionic liquids since they are solids below 100 °C. The melting point for **1** is about 158 °C, whereas compounds **2** and **3** decompose directly at higher temperatures but no melting process is observed below the decomposition temperature. TGA data indicate that all examined compounds show negligible volatility and high thermal stability with a decomposition onset temperature around 300 °C (see Table 1).

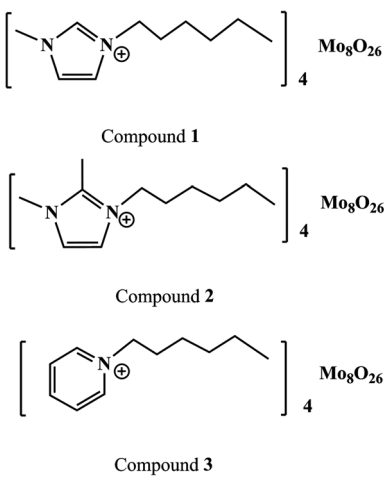

Scheme 1 Structures of compounds **1–3**.

Table 1 Physical property and characterization of compounds **1–3**

Catalyst	Decomp. temp. (°C)	IR (cm^{-1})				
$[Hmim]_4Mo_8O_{26}$	300	946	910	841	710	665
$[Dhmim]_4Mo_8O_{26}$	290	956	911	837	714	650
$[Hpy]_4Mo_8O_{26}\cdot H_2O$	310	947	911	836	717	632

FT-IR spectra were used to clarify the structure of the $Mo_8O_{26}^{4-}$ anions. All three compounds show similar IR spectra with respect to Mo–O bond stretching. The IR spectra exhibit several characteristic Mo–O stretching bands in the region of 700–1000 cm^{-1} (see the data in Table 1). The values are in good accordance with those published in the literature.[16,17] The single-crystal X-ray structures were obtained for compounds **1** and **3**, which further confirm the results of the spectroscopic analysis (Fig. 1 and 2).

A summary of experimental data of the crystal determination can be found in the Experimental section. Selected bond distances of the $Mo_8O_{26}^{4-}$ anions of **1** and **3** are given in Table 2. Both compounds show an array of eight edge-shared MoO_6 octahedra, which includes different types of Mo–O bonds: terminal Mo–O_t, bridging Mo–$O_{\mu 2}$, Mo–$O_{\mu 3}$ and Mo–$O_{\mu 5}$, indicating a typical β-octamolybdate.[17b,18] According to the X-ray structure of compound **1**, the averaged bond distance

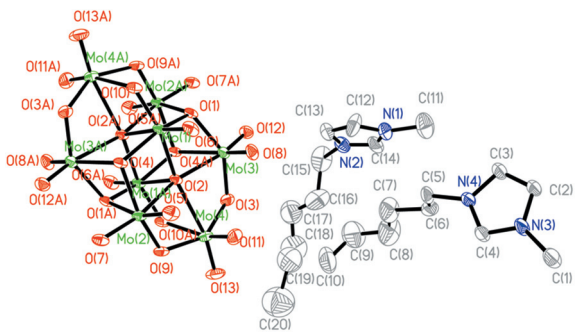

Fig. 1 ORTEP view of compound **1** showing vibrational ellipsoids at the 50% probability level. H atoms are omitted for clarity.

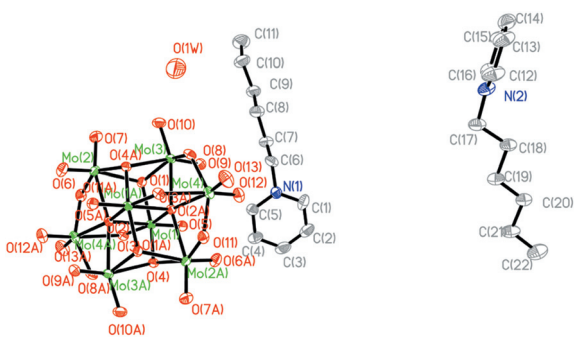

Fig. 2 ORTEP view of compound **3** showing vibrational ellipsoids at the 50% probability level. H atoms are omitted for clarity.

Table 2 Selected bond distances (Å) for compounds **1** and **3**[a]

	$Mo–O_t$		$Mo–O_{\mu2}$		$Mo–O_{\mu3}$		$Mo–O_{\mu5}$	
1	Mo(1)–O(6)	1.693(5)	Mo(1)–O(10)	1.748(5)	Mo(1)–O(4)	1.941(4)	Mo(1)–O(2)	2.136(4)
	Mo(2)–O(5)	1.690(5)	Mo(2)–O(9)	1.892(5)	Mo(1)–O(1)	1.942(5)	Mo(1)–O(2)#1	2.356(4)
	Mo(2)–O(7)	1.698(5)	Mo(3)–O(3)	1.892(5)	Mo(2)–O(4)	2.002(4)	Mo(2)–O(2)	2.334(4)
	Mo(3)–O(12)	1.701(5)	Mo(4)–O(3)	1.926(5)	Mo(2)–O(1)#1	2.332(4)	Mo(3)–O(2)	2.318(4)
	Mo(3)–O(8)	1.704(5)	Mo(4)–O(9)	1.934(5)	Mo(3)–O(1)	2.008(5)	Mo(4)–O(2)	2.455(4)
	Mo(4)–O(11)	1.696(6)	Mo(4)–O(10)#1	2.280(5)	Mo(3)–O(4)#1	2.329(4)		
	Mo(4)–O(13)	1.699(6)						
3	Mo(1)–O(5)	1.694(3)	Mo(1)–O(3)	1.748(3)	Mo(1)–O(4)	1.962(3)	Mo(1)–O(2)#1	2.135(2)
	Mo(2)–O(6)	1.698(3)	Mo(2)–O(11)#1	1.899(3)	Mo(1)–O(1)	1.951(3)	Mo(1)–O(2)	2.352(2)
	Mo(2)–O(7)	1.701(3)	Mo(3)–O(8)	1.882(3)	Mo(2)–O(4)#1	2.002(3)	Mo(2)–O(2)	2.376(2)
	Mo(3)–O(9)	1.701(3)	Mo(4)–O(11)	1.927(3)	Mo(2)–O(1)	2.310(3)	Mo(3)–O(2)#1	2.353(2)
	Mo(3)–O(10)	1.702(3)	Mo(4)–O(8)	1.934(3)	Mo(3)–O(1)	2.001(3)	Mo(4)–O(2)#1	2.388(2)
	Mo(4)–O(13)	1.694(3)	Mo(4)–O(3)#1	2.308(3)	Mo(3)–O(4)#1	2.299(3)		
	Mo(4)–O(12)	1.698(3)						

[a] Symmetry codes: #1 − x, −y, −z + 2 (**1**), #1 − x, −y + 2, −z + 2 (**3**).

for terminal Mo═O is 1.697 Å. The bridging Mo–O–Mo (with two coordinated oxygen) bonds have an averaged distance of 1.911 Å, the triple coordinated oxygen atoms exhibit a Mo–O distance 1.942 Å, the five-coordinated oxygens exhibit an averaged Mo–O bond distance of 2.336 Å. Beside these well-established dominating bond distances, there are some "intermediate" bond lengths of 2.002, 2.008, 2.332, 2.329 and 2.455 Å originating from non-regular three- and five-coordinated oxygen atoms. Anomalous bond distances were obtained for Mo(1)–O(10)–Mo(4) bridge with big variations from 1.748 to 2.280 Å. Possibly the intermolecular interaction with Hmim cations leads to more pronounced variations in Mo–O bond distances than observed in "normal" $[Mo_8O_{26}]^{4-}$ complexes. In aqueous solution, only three different Mo–O bond distances are found, namely 1.70, 1.90 and 2.30 Å for "isolated" $[Mo_8O_{26}]^{4-}$ anions.[19] These values are in good agreement with some of the averaged distances (1.697, 1.911 and 2.336 Å) obtained for compound **1**. These values can be characteristic of the most "regular" basic octahedral units. It is interesting to note that the Mo–O bond stretching vibrations are in an (almost) linear relationship with the Mo–O bond distances. It is known that there are several empirical relations between stretching frequencies (or the derived force constants) and the bond distances. A Badger type of relation exhibits a linear correlation between $(\nu/1000)2$ and $1/r^3$, where ν is the stretching frequency (cm^{-1}) and r is the bond distance (Å). Accordingly, the series of IR bands for compound **1** at 946, 910, 840, 710 and 665 cm^{-1} (Table 1) can be correlated to 1.697, 1.911, 1.942, 2.049 and 2.336 Å Mo–O bond distances, respectively. Very similar conclusions can be drawn for compound **3**, since both the IR spectra and the X-ray structures are very similar to those of compound **1**. Similarly, the Mo–O stretching Raman frequencies of solid $Na_2Mo_2O_7$ at 990 (IR), 939, 925, 881, 821 and 768 cm^{-1} [20] can be correlated to the Mo–O bond distances 1.700, 1.772, 1.832, 1.937, 2.058 and 2.436 Å, respectively.[21] It is further noteworthy that the linear correlation is valid for both the octahedral and tetrahedral units of the anion structure.

Epoxidation of olefins

Compounds **1–3** were examined as catalysts for the epoxidation of different olefins (including cyclooctene, cyclohexene, styrene, 1-hexene and 1-dodecene) using 30% hydrogen peroxide as oxidant. Details concerning the catalytic reaction are given in the Experimental section. Blank reactions show no cyclooctene conversion with excess amounts of H_2O_2 in the absence of catalyst at 60 °C.

The reaction was first carried out by using compound **1** as catalyst and cyclooctene as standard substrate in different solvents, at various temperatures and different amounts of oxidant or catalyst. Data for cyclooctene conversion and epoxide yield can be found in Tables 3 and 4. Data in entries 1–4 and 8 of Table 3 reflect solvent effects on catalytic performance: EtOH- and CH_3CN-mediated reactions resulted in the best conversions and epoxide yields, whereas EtOAc, benzene and toluene only gave a medium or low conversion and yield. It was observed that compound **1** was insoluble in all solvents examined at 60 °C. However, after adding

Table 3 Epoxidation of *cis*-cyclooctene using compound **1** as catalyst

Entry[a]	Solvent	$n_{(H2O2)}$:$n_{(olefin)}$	Conv.[b] (%)	Yield[c] (%)	Temp. (°C)
1	EtOH	1.2	94	92	60
2	EtOAc	1.2	45	44	60
3	Benzene	1.2	11	10[d]	60
4	Toluene	1.2	56	49	60
5	CH_3CN	1.2	51	49	25
6	CH_3CN	1.2	60	57	40
7	CH_3CN	1.2	60	57	50
8	CH_3CN	1.2	90	87	60
9	CH_3CN	1.2	90	87	70
10	CH_3CN	1.0	81	76	60
11	CH_3CN	1.5	98	93	60
12	CH_3CN	2.0	99	97	60

[a] Reaction conditions: *cis*-cyclooctene (2 mmol), $[Hmim]_4Mo_8O_{26}$ (1.5 mol%), solvent (1 mL), t = 1 h. [b] Conversion to cyclooctene oxide was calculated by GC analysis. [c] Isolated yield after column chromatography. [d] Yield was calculated based on GC analysis.

Table 4 Epoxidation of *cis*-cyclooctene with different amounts of compound **1** as catalyst

Entry[a]	Catalyst amount (mol%)	Conv.[b] (%)	Yield[c] (%)
1	0.25	46	31
2	0.5	72	70
3	1	88	83
4	1.5	98	93
5	2	100	98
6	2.5	100	97
7	3	100	98

[a] Reaction conditions: *cis*-cyclooctene (2 mmol), acetonitrile (1 mL), $n_{(H2O2)}$:$n_{(olefin)}$ = 1.5, t = 1 h at 60 °C. [b] Conversion to cyclooctene oxide was calculated by GC analysis. [c] Isolated yield after column chromatography.

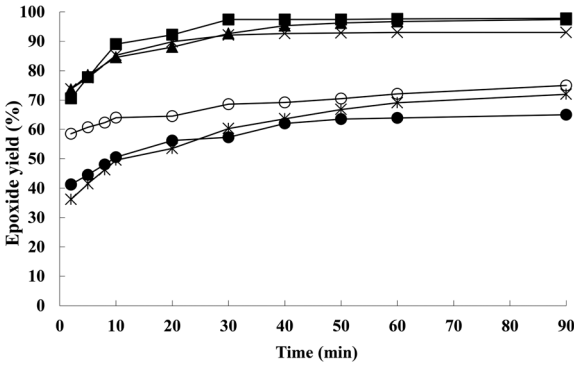

Fig. 3 Time-dependent yield of cyclooctene epoxide in the presence of compounds **1–3** as catalysts at 60 °C with 1.5 mol% (■, **1**; ×, **3**; ▲, **2**) and 0.5 mol% (○, **1**; *, **2**; ●, **3**) catalyst.

1.2 equiv. of H_2O_2 (30%) solution, the white catalyst powder changed its color to yellow (indicating the formation of a reaction product with hydrogen peroxide, most likely the actual catalyst/active species) and dissolved very fast, forming a homogeneous solution when using EtOH and CH_3CN as solvents. In the case of EtOAc, benzene or toluene as solvents, the catalyst could not be dissolved in the organic/water biphasic system which is formed. This results in only a low conversion and epoxide yield. In CH_3CN, a self-precipitation of the catalyst after the completion of reaction took place, similar to the phenomenon observed by Xi *et al.*[13] with respect to $[\pi\text{-}C_5H_5NC_{16}H_{33}]_3[PO_4(WO_3)_4]$ in catalyzed propylene epoxidation. Such catalysts combine the advantages of both homogeneous and heterogeneous reactions. Since the catalyst undergoes a solid–liquid–solid phase transfer during the reaction, it can be easily recycled by filtration.

Based on the advantage of self-separation for the catalyst, CH_3CN was applied as solvent for further studies. In a further set of experiments, the temperature effect on catalytic performance was studied. The reaction at 70 °C exhibits the highest cyclooctene conversion and the best isolated epoxide yield (Table 3, entry 9). The corresponding data are slightly lower at 60 °C. Since the H_2O_2 molecule may decompose faster at higher temperatures, it is nevertheless favorable to carry out the reaction at 60 °C. Entries 8, 10–12 in Table 3 indicate the effect of oxidant amount on catalytic performance. 1.0 to 2.0 equiv. of H_2O_2 to substrate was applied in catalysis. It was observed that a molar equivalent amount of H_2O_2 was not enough to complete the oxidation reaction, while on adding ≥1.5 equiv. of H_2O_2, more than 98% conversion can be achieved. Thus at least 1.5 equiv. of H_2O_2 is necessary to complete the catalytic reaction.

Table 4 shows the effect of the applied catalyst amount on the catalytic performance. In general, the higher the amount of catalyst applied, the higher are conversion and yield. When increasing the catalyst amount up to 2 mol%, the reaction reaches almost 100% cyclooctene conversion, and no diol byproduct was observed in the reactions.

Based on the examination of the catalytic performance for compound **1**, all three compounds were further examined in detail for their catalytic behaviour for cyclooctene epoxidation, with amounts of both 1.5 and 0.5 mol% of catalyst applied. All compounds examined show quite high catalytic activity and selectivity towards cyclooctene epoxide, no diol being observed according to GC analysis. When adding 1.5 mol% of catalysts **1–3** to the system, >70% cyclooctene epoxide was obtained within 2 minutes and *ca.* 96% after 30 minutes. Both compounds **1** and **2** as catalysts lead to almost 100% epoxide yield within 1.5 h. Compound **3** gives an epoxide yield of 93% after 1.5 hours. The turnover frequencies (TOFs) for compounds **1–3** are 622, 621 and 628 h^{-1}, respectively (calculated after 5 min reaction time). Due to similar activity with 1.5 mol% of catalyst, it is difficult to compare the catalyst performance in more detail. Therefore, the system was further examined with a decreased catalyst amount (0.5 mol%). It can be seen from Fig. 3 that compound **1** shows higher activity than compounds **2** and **3** in the initial reaction phase, whereas **1** and **2** result in similar epoxide yields after 1.5 hours. The TOFs with an amount of 0.5 mol% of catalyst are in general higher than that with 1.5 mol% of catalyst, with values of 1488 (**1**), 984 (**2**) and 1080 (**3**) h^{-1} (calculated after 5 min of the reaction). Despite compound **3** displaying a higher TOF than of compound **2**, the final epoxide yield is lower. Moreover, the epoxide yields do not increase after 40 minutes for both amounts of catalyst applied for compound **3**. Similar to compound **1**, compounds **2** and **3** also exhibited a self-separation phenomenon in CH_3CN. It was observed that all the catalyst solid dissolved immediately after adding H_2O_2 to the system at 60 °C; however precipitation occurred already within 10 minutes for each reaction with both 1.5 mol% and 0.5 mol% of catalyst applied, indicating a fast reaction rate and that most H_2O_2 molecules had been consumed within 10 minutes of starting the reaction. As can also be observed from Fig. 3, all the reactions already give quite high epoxide yields after 2 minutes of reaction, and the yields keep increasing rapidly before 10 minutes, and slow down thereafter. Due to the low concentration of H_2O_2 after 10 minutes, the reaction activity decreases significantly and catalyst precipitation occurs.

It is well established that $\{PO_4[MO(O_2)_2]_4\}^{3-}$ (M = Mo, W) is the active species when using $PM_{12}O_{40}^{-}$ based POM as catalyst

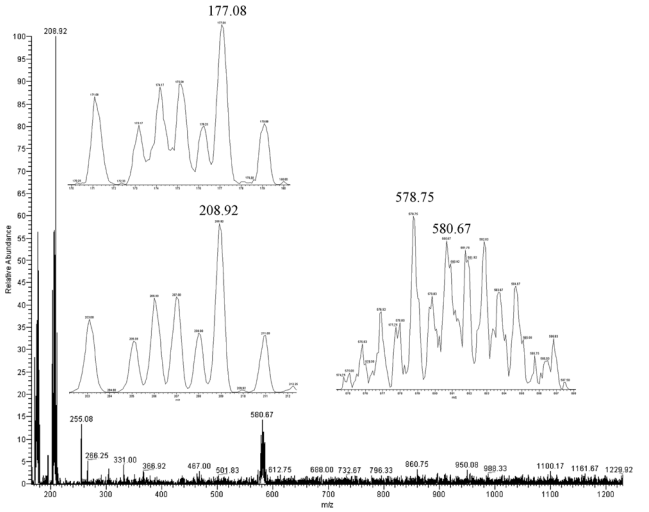

Fig. 4 ESI-MS (negative mode) measurement of the isolated active species.

and H_2O_2 as oxidant for epoxidation.[10] However, not much work has been done on the examination and isolation of catalytic active species for $[Mo_8O_{26}]^{4-}$ anion-based catalysts. Galindo *et al.*[22] successfully isolated a tetraperoxo-octamolybdate derivative with the formula $[Hdmpz]_4[Mo_8O_{22}(O_2)_4(dmpz)_2]\cdot 2H_2O$ as an intermediate during the preparation of the oxodiperoxo species $[MoO(O_2)_2(dmpz)_2]$. Another reported peroxo-octamolybdate is $[NH_4]_4[Mo_8O_{24}(O_2)_2(H_2O)_2]\cdot 4H_2O$.[23] To the best of our knowledge, these are the only two peroxo-octamolybdates reported in the literature. Since the isolation of these intermediates is governed by serendipity, an efficient synthetic route to this compound has still not been established and complex mixtures were obtained in all cases. The reaction between compound **1** and H_2O_2 was studied in order to examine the catalytic species in our work. FT-IR and negative ESI-MS measurements were performed to detect the possible active species towards epoxidation. When adding 30% H_2O_2 to a suspension of compound **1** in acetonitrile at 60 °C, the solid dissolves completely and finally results in a yellow solution, indicating the formation of an active species. Nevertheless, the ionic peak representing the peroxo-octamolybdate could not be detected in the ESI-MS spectra. Instead, a peak indicating the dissociated oxodiperoxomolybdenum species $MoO(O_2)_2$ (m/z = 177.08) was observed, which may be the possible active species in catalysis (Fig. 4).

Fig. 5 shows the IR spectra of compound **1** (5a), after the reaction with excess H_2O_2 (5b), and the recycled compound **1** (5c). It can be observed that the spectrum of the catalyst precursor has Mo=O vibrations at 946 cm^{-1}, and bridging Mo–O–Mo vibrations in the range of 665–910 cm^{-1}. However, after the reaction with excess H_2O_2, the bridging Mo–O–Mo vibration peaks disappear. Instead, a peroxo-bond absorption peak ν(O–O) at 854 cm^{-1} (stretching vibration) can be observed (Fig. 5b).[13a] The disappearance of bridging Mo–O–Mo vibrations further confirms the dissociation of the cluster structure, which is in accordance with the ESI-MS data. Interestingly, the cluster structure of $Mo_8O_{26}{}^{4-}$ is recovered after H_2O_2 is completely consumed. As can be seen from the spectrum of recycled compound **1** (Fig. 5c), no vibrational changes are observed for the recycled compound, indicating good stability of the catalyst.

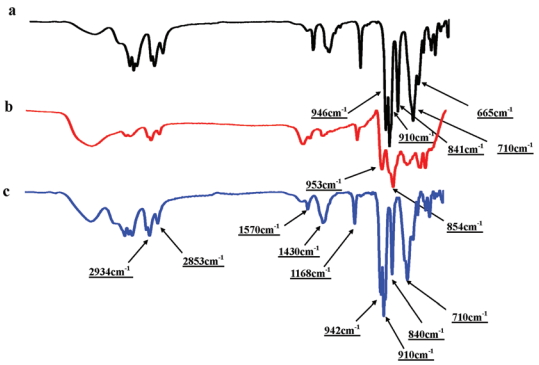

Fig. 5 Infrared spectra of pure compound **1** (a), after the reaction with H_2O_2 (b), and recycled compound **1** (c).

Table 5 Epoxidation of different olefins

Entry[a]	Olefin	Conv.[b] (%)	Yield[c] (%)
1	Cyclohexene	96	44[d]
2	Styrene	100	91[e]
3	1-Hexene	99	96
4	1-Dodecene	91	87

[a] Reaction conditions: *cis*-cyclooctene (2 mmol), $[Hmim]_4Mo_8O_{26}$ (1.5 mol%), acetonitrile (1 mL), $n_{(H2O2)}$:$n_{(olefin)}$ = 1.5, t = 4 h at 60 °C. [b] Conversion to cyclooctene oxide was calculated by GC analysis. [c] Isolated yield after column chromatography. [d] 1,2-Cyclohexanediol was detected as major byproduct. [e] The main product was benzyl aldehyde. The selectivity to styrene oxide was less than 2%.

Besides cyclooctene, the catalytic system was also applied to other olefins (Table 5). Excellent activity for different olefins can also be achieved, even for terminal olefins such as 1-hexene and 1-dodecene. However, a significant amount of diol can be detected in the case of the epoxidation of cyclohexene, while the oxidation of styrene resulted in the formation of benzyl aldehyde as the main product.

Recycling and reuse of compounds 1–3 as epoxidation catalysts

Owing to the self-precipitation feature of the catalysts, compounds **1–3** were recycled directly by filtration after the reaction. Comparing to the recycling process for $[(n\text{-}C_4H_9)_4N]_4[\alpha\text{-}Mo_8O_{26}]$[17a] reported by Deng *et al.*, no additional organic solvent is necessary to precipitate the solid in our system. The recovered solid was just washed with water, and then used directly as catalyst for the next run. The recycling yields for all the catalysts were higher than 95%. The losses are largely ascribed to the workup and may be quantitative after some optimization. Fresh *cis*-cyclooctene and H_2O_2 were then

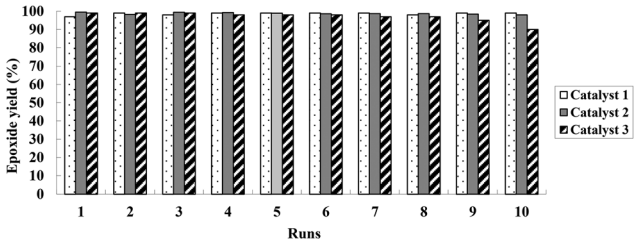

Fig. 6 Reuse of compounds **1–3** for epoxidation of *cis*-cyclooctene at 60 °C.

added for a new reaction cycle. Fig. 6 shows the reuse of compounds **1–3** as catalysts for *cis*-cyclooctene epoxidation at 60 °C with 1.5 mol% of catalysts for 1 hour. Compounds **1** and **2** can be reused for at least ten cycles without significant decrease of yield, proving that this system has persistent activity during the recycling experiments.

Experimental

General methods

All chemicals were purchased from Sinopharm Chemical Reagent Co. Ltd of China or Acros and used without further purification. ^{1}H NMR spectra were recorded with a 500 MHz Bruker Avance DPX-500 spectrometer. IR spectra were recorded with a PerkinElmer Frontier FT-IR spectrometer. Catalytic runs were monitored by GC methods with an Agilent 6890 instrument using a capillary column (30 m × 0.25 mm × 0.25 μm). Microanalyses of the obtained products were performed with a Flash EA 1112 series elemental analyzer. Melting points were determined by an X-6 micro melting point apparatus (Beijing Tech Instrument Co. Ltd). Thermogravimetric analysis (TGA) and differential scanning (DSC) analysis were conducted utilizing a Netzsch-STA 409 PC system, and typically about 10 mg of each sample was heated from 25 °C to 1000 °C at 10 K min^{-1}. ESI-MS spectra were recorded by an LCQ Fleet ESI mass spectrometer. The imidazolium or pyridinium bromine salts were prepared according to the literature.[24]

Synthesis and characterization

Compounds **1–3** were prepared according to the published procedures,[17b] as follows. A solution of $Na_2MoO_4{\cdot}2H_2O$ (4.8 g, 20 mmol) was dissolved in 30 mL of water, and then the solution was acidified with HCl (37%, *ca.* 10 mL) to a pH value of 4.5. The resulting mixture was refluxed for 1 h. After cooling down the solution to room temperature, imidazolium or pyridinium bromine salts (*ca*. 10 mmol) were added and a white solid was precipitated immediately from the solution. After 30 min, the water solution was evaporated to about 5 mL at 100 °C. Then the precipitate was filtered and thoroughly washed three times successively with water and ethanol. Recrystallization of the solid from acetonitrile afforded white crystals.

Characteristic data

Compound **1**: $[C_{10}H_{19}N_2]_4Mo_8O_{26}$ (1852.00). Yield, 81% (white crystal). Elemental analysis calcd: C, 25.93, H, 4.13, N, 6.05; found: C, 25.82, H, 3.98, N, 6.01. IR (KBr, cm^{-1}): see Table 1. ^{1}H NMR (500 MHz, DMSO-d_6, r.t., ppm): δ = 9.13 (s, 1H, mz-H^2), 7.77 (s, 1H, mz-H^4), 7.70 (s, 1H, mz-H^5), 4.18 (t, 2H, CH_2), 3.88 (s, 3H, NCH_3), 1.80 (m, 2H, CH_2), 1.28 (m, 6H, 3 × CH_2), 0.87 (m, 3H, CH_3). ESI-MS (methanol, *m*/*z*, %): cation, 167.1 ($C_{10}H_{19}N_2^+$, 100%).

Compound **2**: $[C_{11}H_{21}N_2]_4Mo_8O_{26}$ (1908.88). Yield, 76% (white crystal). Elemental analysis calcd: C, 27.69, H, 4.44, N, 5.87; found: C, 27.52, H, 4.38, N, 5.88. IR (KBr, cm^{-1}): see Table 1. ^{1}H NMR (500 MHz, DMSO-d_6, r.t., ppm): δ = 7.64 (s, 1H, mz-H^4), 7.61 (s, 1H, mz-H^5), 4.10 (t, 2H, CH_2), 3.75 (s, 3H, NCH_3), 1.70 (m, 2H, CH_2), 1.27 (s, 6H, 3 × CH_2), 0.87 (t, 3H, CH_3). ESI-MS (methanol, *m*/*z*, %): cation, 181.1 ($C_{11}H_{21}N_2^+$, 100%).

Compound **3**: $[C_{11}H_{18}N]_4Mo_8O_{26}{\cdot}H_2O$ (1858.59). Yield, 82% (white crystal). Elemental analysis calcd: C, 28.43, H, 4.01, N, 3.01; found: C, 28.45, H, 3.98, N, 3.04. IR (KBr, cm^{-1}): see Table 1. ^{1}H NMR (500 MHz, DMSO-d_6, r.t., ppm): δ = 9.13 (d, 2H. py-H^{2,6}), 8.62 (t, 1H, py-H^4), 8.17 (t, 2H, py-H^{3,5}), 4.61 (t, 2H, CH_2), 1.91 (m, 2H, CH_2),1.28 (m, 6H, 3 × CH_2), 0.85 (t, 3H, CH_3). ESI-MS (methanol, *m*/*z*, %): cation, 164.1 ($C_{11}H_{18}N^+$, 100%).

General procedure for the epoxidation of olefins

In a typical reaction, compound **1** (55.6 mg, 30 μmol) was applied as catalyst and added to 1 mL of CH_3CN in a reaction vessel in air. Olefin (2 mmol) was added, followed by the addition of H_2O_2 at 60 °C to start the reaction. The course of the reactions was monitored by quantitative GC analysis. Samples were taken at regular time intervals, diluted with acetonitrile, and treated with a catalytic amount of $MgSO_4$ and MnO_2 to remove water and to destroy the unreacted peroxide. The resulting slurry was filtered and the filtrate injected onto a GC column. The conversion of olefins and the formation of epoxides were calculated from calibration curves (r^2 > 0.999) recorded prior to the reaction. For the recycling experiment, the white solid was filtered after cooling down the reaction residue to room temperature. The solid was washed with water 3 times and then dried under vacuum to obtain pure recycled catalyst. Fresh substrate and H_2O_2 were then added for a new reaction cycle.

Single-crystal X-ray structure determinations

Details of the X-ray experiment, crystal parameters, data collections and refinements are summarized in Table 6. Single crystals were mounted on a Bruker XRDR3M/ESYSTCM diffractometer operating at 50 kV and 30 mA equipped with a MoK_α radiation source (λ = 0.71073 Å). Data collections were performed at 273(2) K and 188(2) K with a ω/φ diffraction measurement method and reduction was performed using the SMART and SAINT software with frames of 0.3° oscillation in the θ range 1.5 < θ < 26.2°. The structures were solved by direct

Table 6 Crystal data and structure refinement for compounds **1** and **3**

	1	**3**
Empirical formula	$C_{40}H_{76}N_8Mo_8O_{26}$	$C_{44}H_{74}Mo_8N_4O_{27}$
Formula weight	1852.00	1858.59
Temperature (K)	273(2)	188(2)
Wavelength (Å)	0.71073	0.71073
Crystal system, space group	Monoclinic, $P2(1)/n$	Monoclinic, $P2(1)/n$
Unit cell dimensions	a = 16.3997(11) Å	a = 15.6345 (9) Å
	b = 10.8045(7) Å	b = 12.1211 (7) Å
	c = 17.5797(12) Å	c = 16.5893 (10)Å
	α = 90°	α = 90°
	β = 96.3800(10)°	β = 94.6030(10)°
	γ = 90°	γ = 90°
Volume (Å^3)	3095.7(4)	3133.7(3)
Z, calculated density (mg m^{-3})	2, 1.905	2, 1.970
Absorption coefficient (mm^{-1})	1.645	1.628
F(000)	1680	1836
Crystal size (mm)	0.2 × 0.18 × 0.16	0.23 × 0.17 × 0.10
θ range for data collection (°)	1.80 to 26.04	1.72 to 26.01
Limiting indices	$-20 \le h \le 20$	$-19 \le h \le 17$
	$-12 \le k \le 13$	$-14 \le k \le 14$
	$-20 \le l \le 21$	$-18 \le l \le 20$
Reflections collected/unique	19112/6079 [R(int) = 0.0411]	19651/6162 [R(int) = 0.0390]
Completeness to θ = 26.01° (%)	99.5	99.8
Refinement method	Full-matrix least-squares on F^2	Full-matrix least-squares on F^2
Data/restraints/parameters	6079/30/370	6162/0/381
Goodness-of-fit on F^2	1.041	1.025
Final R indices [$I > 2\sigma(I)$]	R_1 = 0.0539	R_1 = 0.0345
	wR_2 = 0.1392	wR_2 = 0.0720
R indices (all data)	R_1 = 0.0753	R_1 = 0.0460
	wR_2 = 0.1552	wR_2 = 0.0773
Largest diff. peak and hole (e Å^{-3})	1.653 and −1.253	0.658 and −0.458

methods and all non-hydrogen atoms were subjected to anisotropic refinement by full-matrix least-squares on F^2 using the SHELXTL package.[25]

Crystallographic data (excluding structure factors) for the structures reported in this paper have been deposited with the Cambridge Crystallographic Data Centre as supplementary publication nos. CCDC-997672 (**1**) and CCDC-997673 (**3**).

Conclusions

Three [$Mo_8O_{26}^{4-}$]-based polyoxomolybdate salts of general formula [Hmim]$_4Mo_8O_{26}$ (Hmim = 1-hexyl-3-methylimidazolium), [Dhmim]$_4Mo_8O_{26}$ (Dhmim = 1,2-dimethyl-3-hexylimidazolium) and [Hpy]$_4Mo_8O_{26}\cdot H_2O$ (Hpy = 1-hexylpyridinium) have been prepared and used to catalyze the epoxidation of different olefins including cyclooctene, cyclohexene, styrene and 1-octene. They can be used as efficient catalysts when using 30% of H_2O_2 as oxidant and acetonitrile as solvent. In general, octamolybdate-based catalysts exhibit high catalytic performance towards the epoxidation of *cis*-cyclooctene. More importantly, since these insoluble compounds form soluble active species after adding oxidant and are able to self-precipitate after the completion of the reaction, the compounds can be used as self-separating catalysts. Recycling experiments indicate that the catalysts can be recycled and reused at least 10 times without significant loss of activity, indicating good stability of the catalysts. Negative ESI-MS data indicate that the dissociated oxodiperoxo compounds might be the catalytic active species for the epoxidation reactions.

Acknowledgements

M.D.Z. and S.L.Z. thank the National Science Foundation of China (21101085), the National Science & Technology Pillar Program (2012BAF03B02) and the Program for Liaoning Excellent Talents in University (LJQ2012031) for financial support. X.B.L. thanks the "100 Talents" program of Chinese Academy of Sciences (KJCX2-EW-H05) for financial support.

Notes and references

1 K. Weissermel and H. J. Arpe, *Industrial Organic Chemistry*, VCH, Weinheim, 3rd edn, 1997.
2 (*a*) S. Huber, M. Cokoja and F. E. Kühn, *J. Organomet. Chem.*, 2014, **751**, 25–32; (*b*) S. A. Hauser, M. Cokoja and F. E. Kühn, *Catal. Sci. Technol.*, 2013, **3**, 552–561.
3 (*a*) N. Mizuno, K. Yamaguchi and K. Kamata, *Coord. Chem. Rev.*, 2005, **249**, 1944–1956; (*b*) G. Grigoropoulou, J. H. Clark and J. A. Elings, *Green Chem.*, 2003, **5**, 1–7.
4 (*a*) G. Schindler, C. Walsdorff, R. Koerner and H. Goebbel, *WO*, 2007000396, 2007; (*b*) W. Cheng, X. Wang, G. Li, X. Guo and S. Zhang, *J. Catal.*, 2008, **255**(2), 343–346; (*c*) C. Shi, B. Zhu, M. Lin and J. Long, *Catal. Lett.*, 2009, **133** (1–2), 70–75; (*d*) J. Zhuang, G. Yang, D. Ma, X. Lan, X. Liu,

X. Han, X. Bao and U. Mueller, *Angew. Chem., Int. Ed.*, 2004, **116**(46), 6537–6541.

5 (*a*) C. C. Romão, F. E. Kühn and W. A. Herrmann, *Chem. Rev.*, 1997, **97**, 3197–3246; (*b*) F. E. Kühn, A. Scherbaum and W. A. Herrmann, *J. Organomet. Chem.*, 2004, **689**, 4149–4164; (*c*) W. A. Herrmann, A. M. J. Rost, J. K. M. Mitterpleininger, N. Szesni, W. Sturm, R. W. Fischer and F. E. Kühn, *Angew. Chem., Int. Ed.*, 2007, **46**, 7901–7903; (*d*) E. Tosh, J. K. M. Mitterpleininger, A. M. J. Rost, D. Veljanovski, W. A. Herrmann and F. E. Kühn, *Green Chem.*, 2007, **12**, 1296–1298.

6 F. E. Kühn, A. M. Santos and M. Abrantes, *Chem. Rev.*, 2006, **106**, 2455–2475.

7 (*a*) K. R. Jain, W. A. Herrmann and F. E. Kühn, *Coord. Chem. Rev.*, 2008, **252**, 556–568; (*b*) A. Raith, P. Altmann, M. Cokoja, W. A. Herrmann and F. E. Kühn, *Coord. Chem. Rev.*, 2010, **254**, 608–634.

8 (*a*) Q. Zhang, S. Zhang and Y. Deng, *Green Chem.*, 2011, **13**, 2619–2637; (*b*) A. Behr, A. J. Vorholt, K. A. Ostrowski and T. Seidensticker, *Green Chem.*, 2014, **16**, 982–1006.

9 (*a*) N. Mizuno and K. Yamaguchi, *Chem. Rev.*, 2006, **6**, 12–22; (*b*) I. V. Kozhevnikov, *Catalysis by Polyoxometalate*, John Wiley & Sons, Chichester, UK, 2002; (*c*) K. Kamata, K. Yonehara, Y. Sumida, K. Yamaguchi, S. Hikichi and N. Mizuno, *Science*, 2003, **300**, 964–966; (*d*) B. Zhang, S. Li, A. Pöthig, M. Cokoja, S. L. Zang, W. A. Herrmann and F. E. Kühn, *Z. Naturforsch. B: Chem. Sci.*, 2013, **68b**, 587–579; (*e*) L. R. Graser, S. Jürgens, M. E. Wilhelm, M. Cokoja, W. A. Herrmann and F. E. Kühn, *Z. Naturforsch. B: Chem. Sci.*, 2013, **68b**, 1138–1142.

10 (*a*) Y. Qiao and Z. Hou, *Curr. Org. Chem.*, 2009, **13**, 1347–1365; (*b*) Y. Ishii, K. Yamawaki, T. Yoshida, T. Ura and M. Ogawa, *J. Org. Chem.*, 1987, **52**, 1868–1870.

11 (*a*) C. Venturello, E. Alneri and M. Ricci, *J. Org. Chem.*, 1983, **48**, 3831–3833; (*b*) C. Venturello and R. D. Aloiso, *J. Org. Chem.*, 1988, **53**, 1553–1557; (*c*) I. V. Kozhevnikov, G. P. Mulder, M. C. Steverink-de Zoete and M. G. Oostwal, *J. Mol. Catal.*, 1998, **134**, 223–228.

12 (*a*) Y. Leng, J. Wang, D. Zhu, X. Ren, H. Ge and L. Shen, *Angew. Chem., Int. Ed.*, 2009, **48**, 168–171; (*b*) L. Liu, C. Chen, X. Hu, T. Mohamood, W. Ma, J. Lin and J. Zhao, *New J. Chem.*, 2008, **32**, 283–289; (*c*) B. S. Chhikara, R. Chandra and V. Tandon, *J. Catal.*, 2005, **230**, 436–439.

13 (*a*) Z. Xi, N. Zhou, Y. Sun and K. Li, *Science*, 2001, **292**, 1139–1141; (*b*) X. Yang, S. Gao and Z. Xi, *Org. Process Res. Dev.*, 2005, **9**, 294–296.

14 (*a*) H. Li, Z. S. Hou, Y. X. Qiao, B. Feng, Y. Hu, X. R. Wang and X. G. Zhao, *Catal. Commun.*, 2010, **11**, 470–475; (*b*) A. C. Cole, J. L. Jensen, I. Ntai, K. L. T. Tran, K. J. Weaver, D. C. Forbes and J. H. Davis, *J. Am. Chem. Soc.*, 2002, **124**, 5962–5963.

15 I. I. E. Markovits, W. A. Eger, S. Yue, M. Cokoja, C. J. Münchmeyer, B. Zhang, M.-D. Zhou, A. Genest, J. Mink, S.-L. Zang, N. Rösch and F. E. Kühn, *Chem. – Eur. J.*, 2013, **19**, 5972–5979.

16 (*a*) Y. Shi, X. Ren, S. Ren, F. Fu, J. Wang and G. Xue, *J. Chem. Crystallogr.*, 2010, **40**, 985–988; (*b*) T. Dong, F.-W. Chen, M.-H. Cao and C.-W. Hu, *Chem. Res. Chin. Univ.*, 2011, **27**(1), 11–14; (*c*) S. Ikegami and A. Yagasaki, *Materials*, 2009, **2**, 869–875; (*d*) Q. Li, P. Wu, P. Yin, J. Zhang, L. Shi and Y. Wei, *J. Cluster Sci.*, 2010, **21**, 181–186; (*e*) H. Gao, J. i. Yu, J. Du, H. Niu, J. Wang, X. Song, W. Zhang and M. Jia, *J. Cluster Sci.*, 2014, **25**(5), 1263–1272; (*f*) D. Xiao, H. An, E. Wang and L. Xu, *J. Mol. Struct.*, 2005, **738**, 217–225.

17 (*a*) C. Yang, Q. Jin, H. Zhang, J. Liao, J. Zhu, B. Yu and J. Deng, *Green Chem.*, 2009, **11**, 1401–1405; (*b*) M.-L. Guo and H.-Z. Li, *Green Chem.*, 2007, **9**, 421–423; (*c*) S. L. Linguito, X. Zhang, M. Padmanabhan, A. V. Biradar, T. Xu, T. J. Emge, T. Asefaab and J. Li, *New J. Chem.*, 2013, **37**, 2894–2901; (*d*) C. A. Gamelas, P. Neves, A. C. Gomes, A. A. Valente, C. C. Romão, I. S. Goncalves and M. Pillinger, *Catal. Lett.*, 2012, **142**, 1218–1224; (*e*) J. Du, J. Yu, J. Tang, J. Wang, W. Zhang, W. R. Thiel and M. Jia, *Eur. J. Inorg. Chem.*, 2011, 2361–2365; (*f*) C. J. Carrasco, F. Montilla, E. Álvarez, M. Herbert and A. Galindo, *Polyhedron*, 2013, **54**, 123–130.

18 (*a*) W. J. Kroenke, J. P. Fackler Junior and A. M. Mazany, *Inorg. Chem.*, 1983, **22**, 2412; (*b*) E. M. III McCarron, J. F. Whitney and D. B. Chase, *Inorg. Chem.*, 1984, **23**, 3275–3280; (*c*) M. Michalec, K. Stadnicka and S. A. Hodorowicz, *Cryst. Res. Technol.*, 2007, **42**, 91–97.

19 D. G. Lyxel, L. Pettersson and I. Persson, *Inorg. Chem.*, 2001, **40**, 584–592.

20 G. D. Saraiva, W. Paraguassu, M. Maczka, P. T. C. Freire, F. F. de Sousa and J. M. Filho, *J. Raman Spectrosc.*, 2011, **42**, 1114–1119.

21 D. J. Jovanović, I. L. Validžić, M. Mitrić and J. M. Nedeljković, *J. Am. Ceram. Soc.*, 2009, **92**, 2467–2470.

22 M. Herbert, F. Montilla, E. Álvarez and A. Galindo, *Dalton Trans.*, 2012, **41**, 6942–6956.

23 (*a*) A. J. Ward, G. J. Arrow, T. Maschmeyer, A. F. Masters, P. Turner and J. K. Clegg, *Acta Crystallogr., Sect. E: Struct. Rep. Online*, 2009, **65**, i53; (*b*) S. Olson and R. Stomberg, *Z. Kristallogr.*, 1997, **212**, 699.

24 J. G. Huddleston, A. E. Visser, W. M. Reichert, H. D. Willauer, G. A. Broker and R. D. Rogers, *Green Chem.*, 2001, **3**, 156.

25 (*a*) G. M. Sheldrick, *SHELXTL97*, University of Göttingen, Germany, 1997; (*b*) *SMART V5.618 Software for the CCD Detector System*, Bruker Analytical X-ray Systems, Inc., Madison, WI, 1998.

